6614 *Macromolecules* **2009**, *42*, 6614–6623
DOI: 10.1021/ma900969b

Macromolecules
ARTICLE

Preparation, Characterization, and Properties of Novel PSMA−POSS Systems by Reactive Blending

Orietta Monticelli,*,† Alberto Fina,‡ Aman Ullah,† and Panjab Waghmare†

†*Dipartimento di Chimica e Chimica Industriale, Università di Genova and INSTM NIPLAB Centre, via Dodecaneso, 31, 16146 Genova, Italy, and* ‡*Politecnico di Torino - sede di Alessandria and INSTM NIPLAB Centre, viale Teresa Michel, 5, 15121 Alessandria, Italy*

Received May 4, 2009; Revised Manuscript Received July 6, 2009

ABSTRACT: Novel hybrid systems based on styrene−maleic anhydride copolymers (PSMA) and a polyhedral oligomeric silsesquioxane characterized by an amino group as reactive side (POSS-NH_2) have been synthesized by one-step reactive blending. The features of the above materials were compared with those of systems based on polystyrene (PS) or an unreactive POSS in order to highlight the effect of both the reactivity of the silsesquioxane and the polymer matrix functionality on the material final characteristics. FTIR measurements evidenced the occurrence of imidization reaction between the MA group of PSMA and the amino group of POSS molecule, with the consequent formation of a cyclic imide linkage binding POSS to the polymer backbone. This reaction turned out to promote POSS distribution in the polymer matrix, as only the systems characterized by the aforementioned functionalities allowed to obtain a silsesquioxane dispersion at nanometric level. By following the evolution of the system features, in terms of glass transition temperature (T_g), morphology, yield, and crystallinity, with the mixing time, it has been verified that using a T_{mix} lower than POSS melting temperature, a surface reaction at the POSS crystal/polymer boundary occurs, leading to the formation of a very peculiar two-phase structure evolving with time. The two phases have been found to contain different POSS concentrations. Biphasic systems, studied by means of differential scanning calorimetry (DSC) and dynamic mechanical thermal analysis (DMTA), have showed two T_g, depending on the presence of unbound POSS acting as a plasticizer. Films prepared from the systems PSMA−POSS containing low amounts of silsesquioxane (up to 10 wt %) have been found to be completely transparent, while the transparency of those based on higher POSS content has been achieved only after removing the unbound POSS. Indeed, the role of silsesquioxane on surface properties has been assessed by evaluating film wettability.

Introduction

Recently, a wide research interest has been devoted to the preparation of organic/inorganic polymer hybrids, intended as materials made of organic and inorganic moieties coexisting at molecular scale, with very different molecular structures.[1]

Various methods were developed to prepare organic/inorganic polymer hybrids, including sol−gel techniques, copolymerization with hybrid building blocks, and post-treatment of organic polymers.[1,2] This class of materials is currently facing applications in a number of areas, including optics, electronics, mechanics, energy, environment, biology, medicine, catalysis, sensors, etc.[3]

Several organo-functionalized compounds based on silica, silicates, transition metal oxides, carbon, or other inorganic cores were developed.[4,5] Among hybrid organic/inorganic building blocks, polyhedral oligomeric silsesquioxanes (POSS) have attracted a significant research effort. POSS are organic/inorganic molecules, approximately 1−3 nm in size, with general formula $(RSiO_{1,5})_n$ where R is hydrogen or an organic group, such as alkyl, aryl, or any of their derivatives.[6−8] In the literature, POSS have often been referred to as nanoparticles, in analogy with well-known nanofillers such as silica, metal oxides, layered silicates, and hydroxides. However, it is certainly more appropriate to refer to POSS as molecules, given their perfectly defined chemical structure and their peculiar properties, which are very different from those of organo-functionalized nanofillers.

*To whom correspondence should be addressed.

From a general point of view, the incorporation of the thermally robust POSS moiety into organic polymers was found to drastically modify the polymer thermal properties supplying greater thermal stability to the polymer matrix, also allowing the tailoring of the polymer glass transition temperature by tuning the POSS concentration. Moreover, incorporation of POSS molecules is responsible for modifications of the mechanical properties[9−11] as well as reduction of both flammability and heat evolution in combustion.[12,13]

In situ copolymerization of POSS to produce hybrid organic/inorganic polymers with pendent POSS groups has been widely studied both for thermoplastics and thermosets.[14−16] Different synthetic routes have been developed, including free radical polymerization, polyaddition, polycondensation, and ring-opening metathesis polymerization.[17] POSS grafting onto a preformed copolymer was also obtained in solution, by POSS hydrosilylation on poly(styrene−butadiene−styrene) copolymer,[18] by coordination bonding on styrene/vinyldiphenylphosphine oxide copolymer,[19] or by hydrogen-bonding between diamidopyridine-functionalized POSS and thymine-functionalized copolymer.[20]

In the latter years, some work has been also carried out on the preparation of polymer−POSS systems by melt blending techniques, these being very appealing, economic, and environmentally friendly processes for the industrial development of POSS technology. Fu et al. first reported melt blending of POSS into polypropylene (PP) and ethylene−propylene (EP) copolymer, showing POSS effects on crystallization and rheological behavior.[21,22] Fina et al. reported melt blending of POSS bearing

 Published on Web 07/14/2009

different alkyl chain lengths (from methyl to octyl) with polypropylene (PP), showing substantial differences in the morphology of the composites by increasing alkyl chain length from octamethyl-POSS to octaisobutyl-POSS as well as on POSS loading.[23]

Zhao et al. used melt blending to prepare various POSS/polycarbonate (PC) systems, which showed differences in compatibility depending on the filler specific structure; namely, trisilanol POSS molecules generally provided better compatibility with PC than fully saturated cage structures, and phenyl-substituted POSS was more compatible with PC than the corresponding isoctyl-substituted molecule.[24]

On the basis of the results reported above, it turns out that, despite silsesquioxane organic functionalization, nanodispersion of POSS into organic polymers at a molecular level is not an obvious achievement; in order to successfully prepare nanostructured POSS/polymer blends, the control of chemical and physical interactions between the organic matrix and the nanofiller is crucial.[25] Thanks to POSS versatility, the possibility to perform a chemical reaction between POSS and a suitable polymer to prepare POSS/polymer hybrids by a one-step melt blending process is a fascinating way to improve polymer properties or to obtain new functionalities. However, the application of reactive blending methods to POSS systems is still in its infancy.

Attempts to prepare poly(ethylene terephthalate) (PET), using differently functionalized POSS, by reactive blending were the first to be reported. Epoxy-trifunctionalized cyclopentyl POSS showed phase separation when melt blended with PET, evidencing a limited extent of the reaction with the polymer.[26] On the other hand, both isoctyl POSS and trisilanol isoctyl POSS showed no phase separation and led to increased modulus at high temperature, especially for the trisilanol POSS, which is potentially reactive on PET chain ends.[27] Zhou et al. reported the reactive blending preparation of PP/octavinyl POSS by free radical reaction, showing that POSS has better compatibility with PP when blended in the presence of a free radical initiator, due to partial POSS grafting onto PP chains.[28] Both mechanical properties and crystallization behavior were strongly affected by bound POSS, which led to a higher modulus and to a relevant increase of nucleation rate.[29] Moreover, an increase of viscosity with increasing POSS content and a solidlike rheological behavior at low frequency when POSS content was higher than 1 wt % were found.[30]

POSS grafting on PP was also explored by in situ γ-ray radiation on previously prepared PP/monofunctional methacryl POSS blends, showing an increase of mechanical properties with both the increase of POSS content and the increase in absorption dose up to 5 kGy.[31]

Most recently, Fina et al. reported successful grafting of monofunctional POSS onto maleic anhydride-grafted PP (PPgMA), taking advantage of the amino-anhydride reaction in a one-step reactive blending process.[32] POSS-grafted PPgMA showed advantages in terms of higher thermal stability and improved mechanical properties with respect to the nonreactive PPgMA/POSS system. Nevertheless, the low content of grafted maleic anhydride in commercial PPgMA limited the amount of graftable POSS. Theoretically speaking, the use of maleic anhydride copolymers could clearly overcome the above drawback. On these grounds, the present paper addresses the preparation of novel poly(styrene-*co*-maleic anhydride) (PSMA)/POSS hybrids by one-step melt blending and their chemical and physical characterization.

Experimental Section

Materials. Octaisobutyl-POSS (referred as POSS in the following) and aminopropyl heptaisobutyl-POSS (referred as POSS-NH_2 from now on) were purchased from Hybrid Plastics as crystalline powders and used as received. Chemical structures for POSS (M = 873.6 g/mol) and POSS-NH_2 (M = 917.6 g/mol) are reported in Figure 1. ^{1}H NMR (ppm) (300 MHz, $CDCl_3$) of POSS-NH_2: δ 2.73 (2H, s, $-CH_2NH_2$), 2.66 (2H, t, $-CH_2CH_2$-NH_2), 1.85 (7H, $-CH_2CH(CH_3)_2$), 1.53 (2H, q, $-CH_2CH_2$-CH_2), 0.96 (42H, dd, $-C(CH_3)_2$), 0.60 (2H, t, $-SiCH_2CH_2$), 0.60 (14H, dd, $-SiCH_2CH$).

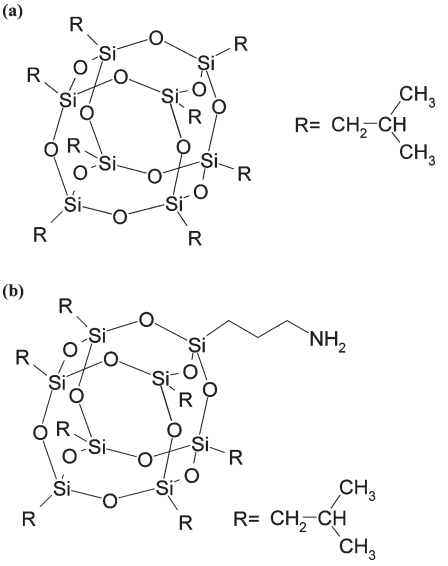

Figure 1. (a) Octaisobutyl-POSS (POSS) and (b) aminopropyl heptaisobutyl-POSS (POSS-NH_2).

Polystyrene-*co*-maleic anhydride (PSMA) (Dylark 332), kindly supplied by Nova Chemicals, was characterized by a concentration of maleic anhydride of 14 mol %, verified by NMR measurements.

Polystyrene (PS), with average molecular weight M_w 230 000 and MFI 7.5 g/10 min (200 °C/5 kg), was purchased from Sigma-Aldrich.

PSMA/POSS System Preparation. PSMA/POSS systems were prepared by mixing the neat polymer and POSS, both octaisobutyl and aminopropyl heptaisobutyl, at various concentrations, from 5 to 50 wt %, in a laboratory internal mixer (240 °C) provided with a mechanical stirrer (Heidolth, type RZR1), applying variable mixing time (t_{mix}), typically using a t_{mix} of 10 min.

Neat PSMA was processed and characterized under the same conditions as reference material. The same equipment and similar conditions (240 °C, 10 min) were applied for the preparation of composite systems based on PS and POSS-NH_2. Materials are identified in the text with the format polymer type/POSS type(concentration)mixing time, e.g., PSMA/POSS-NH_2(20)10.

In order to evaluate the grafting yield, after melt blending all solid samples were broken in small pieces and unreacted POSS was removed by Soxhlet extraction with petroleum ether for 48 h. The grafting yield was calculated by weighting composite samples before and after the above treatment.

Film Preparation. Solutions were prepared by dissolving PSMA or composite systems in acetone (25 wt %) at room temperature. Dense films, characterized by a thickness of ca. 200 μm, were obtained by evaporating the acetone from the cast solution along an overnight exposure in an oven at 110 °C.

SEM. A Leica Stereoscan 440 scanning electron microscope equipped with a backscattered electron detector was used to examine the composite sample morphologies and Si distribution. The specimens were submerged in liquid nitrogen for 30 min and fractured cryogenically. All samples were thinly sputter-coated with carbon using a Polaron E5100 sputter coater.

TEM. Transmission electron microscopy analyses were performed with a high-resolution equipment (JEOL 2010). The measurements were carried out using an accelerating voltage of 200 kV. Ultrathin sections of about 100 nm thick were cut with a Power TOMEX microtome equipped with a diamond knife and placed on a 200-mesh copper grid and stained with ruthenium tetraoxide to obtain sufficient phase contrast.

WAXD. Wide-angle X-ray diffraction was carried out on a Philips PW 1830 powder diffractometer (Ni-filtered Cu Kα radiation).

DSC. Differential scanning calorimetry was performed under a continuous nitrogen purge on a Mettler calorimetric apparatus, model TC10A. Both calibrations of heat flow and temperature were based on a run in which one standard sample (indium) was heated through its melting point. Samples having a mass between 2.5 and 11 mg were used. Data were gathered using a scan rate of 10 °C/min.

^{1}H NMR. NMR spectra were obtained on a Varian 300 NMR, preparing the samples in $CDCl_3$.

DMTA. Dynamic mechanical thermal analysis was performed on a TA Q 800 instrument in tensile mode at an oscillatory frequency of 1 Hz with applied deformation of 0.05% and static load equal to 125% of dynamic load. Temperature scans between 0 and 140 °C were performed at 2 °C/min heating rate. Temperature for T_α relaxation is taken from the maximum of loss modulus (E''). Specimens sizing approximately $30 \times 6 \times 0.2$ mm were cut from films obtained by solvent casting.

FT-IR. Fourier transform infrared spectroscopy spectra were recorded by a Bruker IFS66 spectrometer. The KBr pellet were prepared by mixing the sample with KBr powder (around 1:100) and using a hydraulic press at the pressure of 10 tons. All the samples were dried at 120 °C for 4 h under inert atmosphere and were scanned in the range 400−4000 cm^{-1} with nitrogen purge.

Contact Angle Measurements. Contact angle measurements were performed at room temperature with an Erma G-1 contact angle meter by using pure water as probe liquid.

Results and Discussion

As mentioned in the Experimental Section, the systems PSMA/POSS have been prepared by mixing the polymer matrix with silsesquioxane molecules characterized by an amino group as reactive side in an internal mixer at 240 °C, typically for 10 min. The choice of the mixing temperature was mainly due, on one hand, to the need for acceptably low polymer viscosity during the process and from the other to prevent POSS evaporation, which was found to start at temperatures close to POSS T_m.[33,34] It is worth noticing that the highest POSS content in the reaction mixture, i.e., ∼50 wt %, corresponds to the complete saturation of maleic anhydride group in PSMA.

Moreover, also an unreactive POSS (octaisobutyl-POSS) has been mixed with PSMA, as a reference, in order to highlight the effect of the reactivity of the silsesquioxane on the material final characteristics. Similarly, the influence of the polymer matrix functionality has been investigated by studying the features of samples based on PS and POSS-NH_2.

IR Characterization. In order to study the kind of interactions and/or reactions occurring between the components of the system PSMA/POSS-NH_2, neat PSMA, the amino-type POSS, and the prepared composites have been analyzed by FT-IR measurements. In Figure 2, IR spectra of PSMA, POSS-NH_2, and of the sample PSMA/POSS-NH_2(20)10, based on 20 wt % of POSS-NH_2, are reported.

The neat POSS shows a strong Si−O−Si stretching absorption band at ca. 1100 cm^{-1}, which is the typical absorption peak of the silsesquioxane inorganic framework. PSMA holds two characteristic absorption peaks at 1772 and 1850 cm^{-1} due to symmetric and antisymmetric

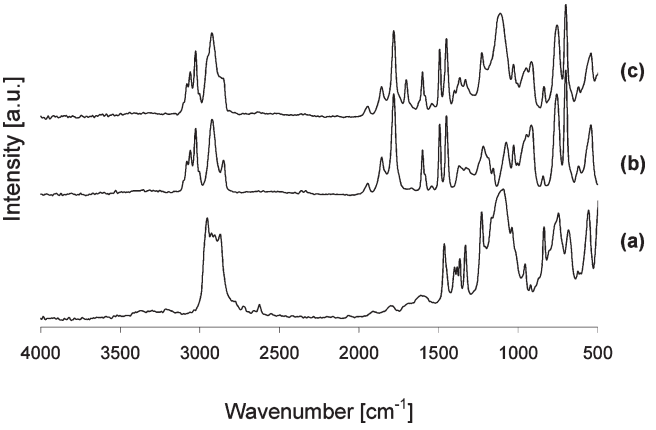

Figure 2. FTIR spectra of (a) POSS-NH_2, (b) PSMA, and (c) PSMA/NH_2(20)10. The curves are shifted vertically for clarity.

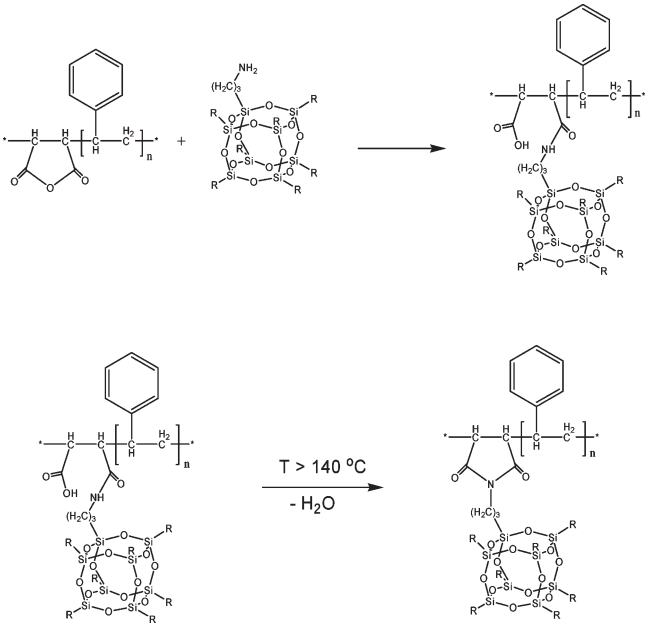

Figure 3. PSMA and POSS-NH_2 reaction scheme.

stretching vibrations of the anhydride carbonyl group as well as a peak at 1213 cm^{-1} attributed to the stretching vibration C−O−C of maleic anhydride units.

In the spectrum of PSMA/POSS-NH_2 systems, together with the peaks characteristics of the neat polymer matrix, two new bands at ca. 1100 and 1700 cm^{-1} appear with intensity proportional to POSS-NH_2 loading. The former band, as previously reported, is due to Si−O−Si stretching vibration and gives evidence of the presence of POSS in the polymer matrix, whereas the one at higher wavenumbers (1700 cm^{-1}) can be assigned to imide groups.[35] It is worth underlining that the intensity of the this latter peak does not disappear in the samples after extraction of unbound POSS, evidencing the occurrence of a grafting reaction between the silsesquioxane molecules and the polymer. Thus, as illustrated in Figure 3, these results prove the occurrence of the imidization reaction between the MA group of PSMA and the amino group of POSS molecules, with the consequent formation a cyclic imide linkage.

It is relevant to point out that both PS/POSS-NH_2 and PSMA/POSS systems do not show the imide peak, while the Si−O−Si stretching absorption is completely removed after the extraction of unbound POSS.

Table 1. Characteristics of the Samples Prepared Using a t_{mix} of 10 min

sample code	type of polymer	type of POSS	POSS concn (wt %)	yield (%)	T_g bw[a] (°C)	T_g aw[b] (°C)
PSMA	PSMA				134	
PSMA/POSS(5)10	PSMA	POSS	5	0	134	134
PSMA/POSS(20)10	PSMA	POSS	20	0	134	135
PS	PS				104	
PS/POSS-NH_2(5)10	PS	POSS-NH_2	5	0	103	104
PS/POSS-NH_2(20)10	PS	POSS-NH_2	20	0	104	104
PSMA/POSS-NH_2(2.5)10	PSMA	POSS-NH_2	2.5	100	133	133
PSMA/POSS-NH_2(5)10	PSMA	POSS-NH_2	5	100	133	135
PSMA/POSS-NH_2(10)10	PSMA	POSS-NH_2	10	80	134	135
PSMA/POSS-NH_2(20)10	PSMA	POSS-NH_2	20	50	121, 135	134
PSMA/POSS-NH_2(50)10	PSMA	POSS-NH_2	50	22	124, 131	135

[a] Measurements carried out before washing the sample. [b] Measurements carried out after washing the sample.

Calculation of Reaction Yield. In order to define the amount of POSS chemically bound to the polymer matrix, the reaction yield has been evaluated by weighting the sample before and after the treatment with a solvent capable to completely solubilize POSS molecules. Indeed, this parameter can provide useful information about the kinds of interactions occurring between the two system components. The yield of the various samples prepared, i.e., the relative amount of POSS retained by the polymer matrices, is given in Table 1.

On the basis of the above results, the following remarks can be drawn. At first, in the case of the samples based on PSMA/POSS and PS/POSS-NH_2, the extraction treatment removes the whole POSS, thus pointing at weak interactions between the polymer and POSS when no chemical reaction occurs as well as at the efficiency of the experimental procedure for the extraction of unbound silsesquioxanes. Conversely, in the systems based on PSMA and POSS-NH_2 the reaction yields vary, being 100% for the samples based on the lowest silsesquioxane content (PSMA/POSS-NH_2(2.5)10 and PSMA/POSS-NH_2(5)10) and decreasing with the increase of POSS loading.

The interpretation of these results has to be accomplished by taking into account also the morphological characterization data discussed in the following.

Morphological Characterization. SEM investigation, coupled to EDS analysis, allowed to study the morphology of the various organic−inorganic systems prepared, paying specific attention to Si dispersion, i.e., POSS distribution, in the polymer matrix. Figure 4a shows the micrograph obtained by backscattering emission (BS) of the sample PSMA/POSS-NH_2(20)10, containing 20 wt % of POSS-NH_2 and prepared by applying a mixing time of 10 min.

No POSS aggregates have been observed on the sample surface, while the elemental analysis has shown a uniform Si distribution without any visible aggregates, thus evidencing a submicrometer POSS dispersion. Similar results have also been obtained with the other samples, even those based on 50 wt % of POSS-NH_2, prepared by using the same t_{mix}.

For comparison, the micrograph of PSMA/POSS(20)10 prepared by mixing octaisobutyl-POSS with PSMA is shown in Figure 4b. The sample is characterized both by the presence of micrometer-sized POSS crystals and by some holes distributed on the polymer surface, left by POSS crystals removed during sample preparation (fragile fracture), giving evidence of the scarce adhesion of POSS to PSMA. A similar POSS aggregation has been found also in the case of composites based on PS and POSS-NH_2.

These results point out that the reactivity between POSS and the polymer matrix is essential to attain nanostructured material. Namely, the reactivity between amino and anhydride groups in the molten polymer, confirmed by FT-IR measurements, turns out to drive POSS nanometric dispersion in the polymer matrix. Besides SEM analysis, X-ray characterization can provide additional information on POSS dispersion and give, since the first pioneering studies on polymer/POSS composites, insights into the system microstructure.[36−38]

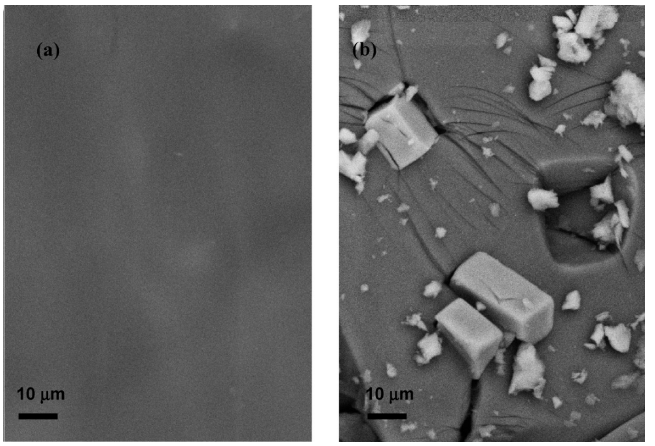

Figure 4. SEM micrographs by BS emission of (a) PSMA/POSS-NH_2-(20)10 and (b) PSMA/POSS(20)10.

Figure 5 shows the WAXD patterns of the neat POSS-NH_2, of PSMA, and those of the hybrid systems prepared by melt blending (PSMA/POSS-NH_2(5)10, PSMA/POSS-NH_2(20)10, PSMA/POSS-NH_2(50)10, and PSMA/POSS-(20)10).

Considering Figure 5, it comes out that POSS-NH_2 is highly crystalline and shows strong reflections at 2ϑ of 7.9° (11.2 Å), 8.0° (11.0 Å), 8.8° (10.0 Å), 11.7° (7.56 Å), and 19.9° (4.44 Å). Conversely, neat PSMA exhibits a typical amorphous pattern. The WAXD profile of PSMA/POSS(20)10 prepared by mixing PSMA with neat isobutyl-POSS shows the diffraction peaks of POSS crystals, thus evidencing that the crystalline organization of silsesquioxane molecules is not affected by the polymer matrix and no molecular dispersion of POSS is obtained, in agreement with morphological characterization results.

On the other hand, WAXD profiles of the samples PSMA/POSS-NH_2(5)10, PSMA/POSS-NH_2(20)10, and PSMA/POSS-NH_2(50)10, containing 5, 20, and 50 wt % of POSS-NH_2, respectively, turned out to be similar to that of neat PSMA, indicating the disappearance of POSS crystalline structure in the composite systems. However, by comparing the portion of the WAXD spectra between 0° and 15° of 2ϑ of the neat polymer matrix with those of PSMA/POSS-NH_2,

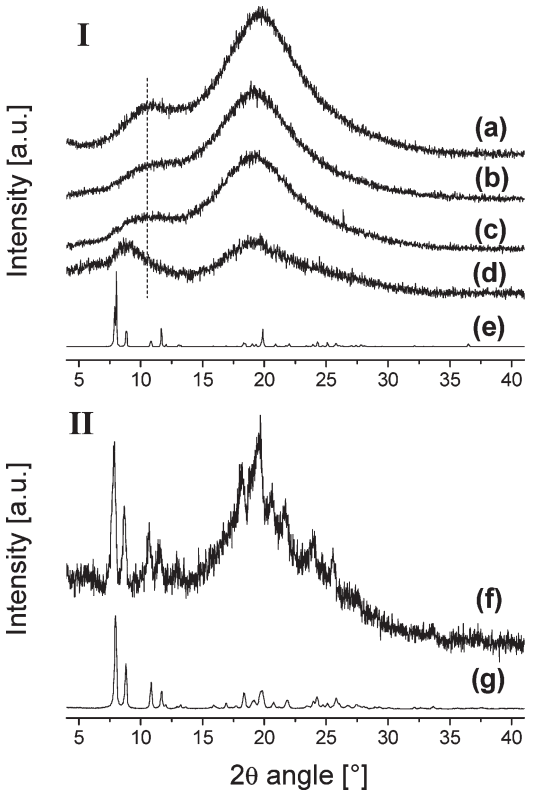

Figure 5. X-ray diffraction patterns of (a) PSMA, (b) PSMA/POSS-NH_2(5)10, (c) PSMA/POSS-NH_2(20)10, (d) PSMA/POSS-NH_2(50)10 (e) POSS-NH_2, (f) PSMA/POSS(20)10, and (g) POSS. The curves are shifted vertically for clarity.

some differences can be noticed, being particularly significant for the higher POSS content samples (PSMA/POSS-NH_2(20)10 and PSMA/POSS-NH_2(50)10). Indeed, for these systems, the above band centered at about 10° for PSMA shifts at lower diffraction angles with respect to that of PSMA, and it turns out to become sharper, especially in the case of PSMA/POSS-NH_2(50)10, as shown in Figure 5. This finding underlines some degree of short-range aggregation of POSS molecules with periodicity in the range of about 10 Å, comparable with crystalline distances described above. Nevertheless, the significant width of this signal suggests very limited aggregation capability for POSS, either grafted on polymer chains or dispersed into the matrix. In the literature, the crystalline structure of POSS as well as that of the polymer matrix turned out to be greatly modified in other POSS/polymer systems. Indeed, as far as POSS copolymers are concerned, Zhen et al.[39] reported that POSS units incorporated as pendant groups to PE backbone aggregated as nanocrystals with an anisotropic crystalline shape, lowering the crystallinity of PE. In the case of poly(ethylene glycol) end-capped at both ends by monofunctional POSS molecules (amphiphilic POSS telechelics), silsesquioxane moieties were found to aggregate and crystallize as nanocrystals disrupting PEO crystallinity.[40] The investigation of the crystalline structure of the system based on poly(butadiene) and POSS, bearing a polymerizable norbornene group, showed the formation of two-dimensional lamellar-like nanostructures of assembled cubic silsesquioxanes.[41]

All the above examples point out that POSS units, attached to the polymer backbone, are still able to cluster to some degree in both the case of semicrystalline and amorphous polymer matrices. On the other hand, in other cases, POSS molecules were found not to be able to organize themselves.

Recently, Seurer et al.[42] found that the aggregation of POSS in ethylene−propylene−POSS terpolymers depended on silsesquioxane peripheral groups. Indeed, POSS characterized by isobutyl or ethyl peripheries turned out not to aggregate.

Elsewhere, the disappearance of typical POSS X-ray peaks in the composite systems constituted of organic/inorganic triblock copolymer poly(styrene−butadiene−styrene) (SBS), containing grafted POSS molecules, was considered as the proof of silsesquioxane dispersion in the polymer matrix by grafting.[43] Moreover, it is relevant to underline that also in the case of some systems prepared by melt blending POSS units were found to lose their crystalline structure as a consequence of their dispersion in the polymer matrix.[44]

On the basis of the experimental results obtained and in the light of the literature findings described above, it is assumed that the broad band partially overlapped to the low-angle PSMA halo points out clustering of either grafted POSS or/with unbound POSS dispersed in the polymer matrix to form very fine aggregates, unable to produce significant diffraction signals. A second possible explanation involves the modification of short-range order for PSMA due to the presence of some POSS moieties in between polymer chains.

Some of the samples prepared have been characterized by TEM analysis in order to accurately evaluate the nanostructure. Indeed, in TEM imaging POSS domains should be darker than the polymer matrix because of their higher mass contrast in comparison with PSMA chains and their crystalline structure. Nevertheless, as previously reported,[45] in order to enhance the contrast between polymer and POSS, TEM sections were stained with RuO_4 vapor, which was found to stain selectively POSS moiety. The micrograph shown in Figure 6a highlights that PSMA/POSS-NH_2(5)10, based on 5 wt % of POSS-NH_2, is characterized by a homogeneous structure, which does not show any appreciable inhomogeneity even at the nanoscale level.

It is relevant to underline that the compositional homogeneity of nanostructured materials such as nanocomposites based on PA6,[46] PS,[47] epoxy,[48] and silicone resins[49,50] was attributed to the formation of hybrid systems, namely to the direct incorporation of POSS units as pendant groups to polymer backbone.

Figure 6b shows the micrograph of the sample PSMA/POSS-NH_2(20)10 prepared by adding 20 wt % of POSS-NH_2 to the reaction mixture. Differently from the previously described composite, the above sample turns out to have a heterogeneous microstructure with a phase segregation typical of immiscible polymer blends.[20−22] As confirmed by EDS analysis, the continuous phase, which represents the picture background and appears darker in Figure 6b, is characterized by a significantly higher concentration of POSS than the globular structure which is pale gray in the above TEM micrograph. To the best of our knowledge, no report so far on POSS−polymer systems have described such kinds of structures.

Taking into account the grafting yield results, it seems reasonable to assume that the phase rich in Si contains both polymer chains highly grafted with POSS and unbound POSS nanodispersed in such highly grafted PSMA, which is expected to be significantly more compatible with POSS as compared to the pristine PSMA. Conversely, as supported by EDS analyses, the pale gray part of the TEM micrograph should correspond to the fraction of the polymer containing

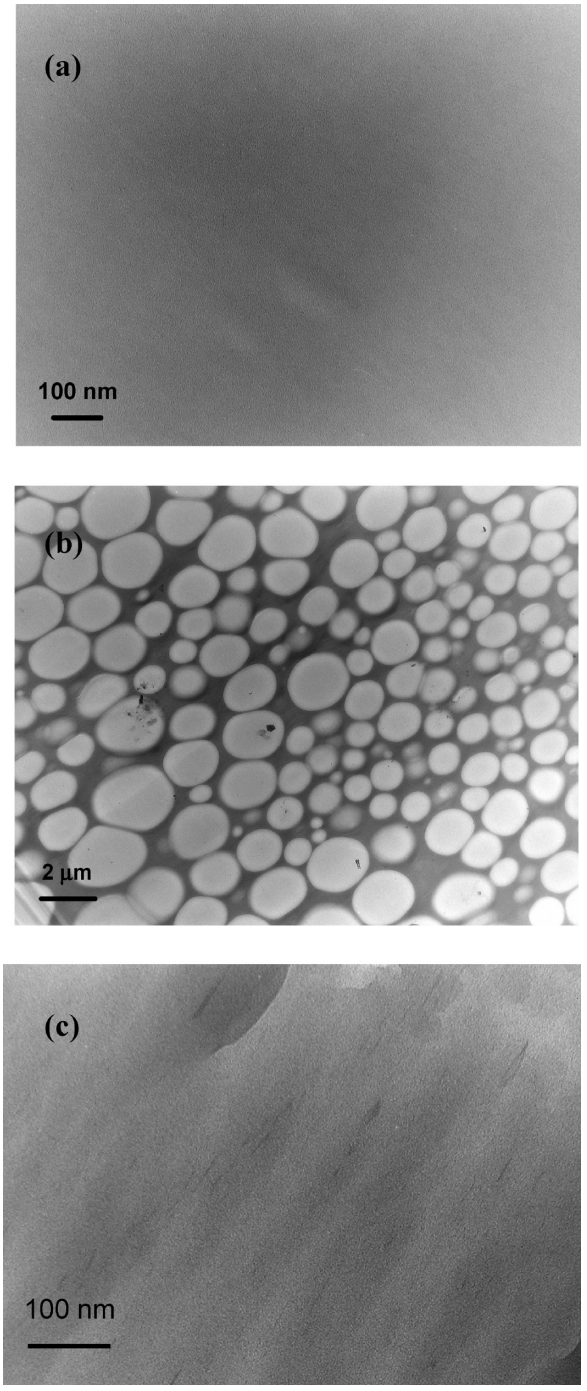

Figure 6. TEM micrographs of (a) PSMA/POSS-NH_2(5)10, (b) PSMA/POSS-NH_2(20)10, and (c) PSMA/POSS-NH_2(20)10 after washing.

a much lower content of POSS. Further results useful for the interpretation of PSMA/POSS-NH_2 microstructure can come both from the study of blends prepared by applying different mixing times and from the evaluation of composite morphology after the treatment to remove unbound POSS. Indeed, as far as this latter aspect is concerned, Figure 6c shows TEM micrograph of PSMA/POSS-NH_2(20)10, which underwent a washing treatment. Conversely to the pristine composite, the material shows no phase separation but some lamellar-like structures distributed in the polymer, characterized by a high concentration of Si. This finding points out that the washing treatment promotes the composite reorganization and proves that the two-phase structure is actually due to unbound POSS. Indeed, as previously mentioned, the formation of similar nanostructures were found also in the case of copolymers based on polybutadiene and POSS.[36] As reported for the above hybrids, also in the case of our systems, this peculiar lamellar morphology might be created by the self-assembling of POSS, namely by the organization of silsesquioxane molecules grafted to the polymer backbone. Clearly, it is of outmost relevance the formation of such nanostructures, which resemble those of clay nanocomposites.[51]

Thermal Characterization. As widely reported, among the polymer features affected by POSS, both physically dispersed or chemically attached to the macromolecules, is the thermal behavior. On this basis, the polymer/POSS systems prepared have been investigated by DSC analysis. An endothermic peak at ca. 260 °C, due to POSS melting, appears in the thermograms of the two unreactive systems (PS/POSS-NH_2 and PSMA/POSS). These findings further support the previously described characterization results, showing the presence of POSS crystals. On the other hand, no POSS melting trace is observed for any of the PSMA/POSS-NH_2 blends.

The glass transition temperatures of the composites, obtained by DSC measurements, are given in Table 1 and compared to those of the neat polymer matrices. By analyzing these results, it comes out that a modification of T_g with respect to those of the neat polymer matrices occurs for the samples based on PSMA and high concentration of POSS-NH_2. Indeed, PSMA/POSS-NH_2(20)10 and PSMA/POSS-NH_2(50)10, containing 20 and 50 wt % of POSS, show two glass transition temperatures, one around 134 °C, corresponding to that of PSMA, and the other at a lower temperature. Interestingly, the latter T_g disappears after the washing treatment to extract unbound POSS.

Variable trends of T_g vs POSS content were reported for different polymer/POSS systems, depending on both the nature of the polymer and the organic substituents on POSS. For copolymers such as poly(norbornene-*co*-norbornene POSS)[6,52] and cyclopentyl POSS containing epoxy resin[53] an enhancement of glass transition temperature, generally ascribed to the hindering of polymer chain mobility of POSS cages, was reported. On the other hand, a decrease of T_g was found, with respect to homopolymers, in POSS containing poly(4-methylstyrene) nanocomposites.[54] Also, epoxy/POSS nanocomposites with 25% of POSS content showed a lower T_g compared to the neat epoxy resin.[55] It was argued that the T_g depression could be connected to incomplete curing reaction because of the inclusion of POSS cages. In the case of poly(hydroxystyrene-*co*-vinylpyrolidone-*co*-isobutylstyryl polyhedral oligosilsesquioxane)[56] the lower T_g of the hybrids, as the POSS concentration increased, was ascribed to the fact that the interactions between copolymers reduced the original dipole−dipole interaction within the polymers.

Wu et al.[57] prepared POSS/PS hybrids by the polymerization of styrene monomer with monofunctional styryl-POSS characterized by seven inert isobutyl (*i*-Bu) groups and found a decrease of glass transition temperature with increasing the silsequioxane concentration. Indeed, the explanation was that the copolymers have the polystyrene backbone randomly branched by *i*-Bu-POSS, which increases the distance between adjacent backbone chains leading to an higher free volume. Also in the case of inorganic−organic hybrid made of POSS-containing methacrylate-based polymer, the lower glass transition temperatures, found upon the incorporation of POSS cages into the polymer structures, was ascribed to the higher free volume induced by the presence of silsesquioxane molecules.[58]

In this light, it is possible to suggest that in POSS-modified polymers there could be competitive factors to determine the glass transition temperature of the resulting materials. Indeed, although the hindering effect of Si−O−Si cages on polymer chain motion may enhance the glass transition temperature, the inclusion of the bulky and flexible organic group on POSS could give rise to an increase of the system free volume, reducing the self-association of the homopolymer molecules and consequently lowering T_g. As far as the systems addressed in this paper are concerned, in those with lower POSS contents and characterized by a high grafting yield, the above effects seem to counterbalance each other, resulting in a T_g similar to that of the neat polymer matrix. Nevertheless, in the case of the samples containing high POSS content, the peculiar two-phase structure has to be considered. Indeed, for the systems with incomplete grafting, also the effect of silsesquioxane which is not directly linked to the polymer backbone but rather finely dispersed in the polymer matrix has to be taken into account as, being able to interact somehow with grafted POSS molecules, it could influence the material final features. Namely, it is reasonable to assert that unbound silsesquioxane reduces the interactions among the macromolecules (either POSS-grafted or not) and, playing a plasticization effect, is able to decrease the material glass transition temperature. Indeed, this model is consistent with the fact that elimination of the unbound POSS fraction gives rise to the disappearance of the lower temperature T_g. Clearly, the higher temperature T_g at ca. 134 °C remains unchanged after the extraction treatment, corresponding to PSMA/POSS-NH_2 as discussed above for the lower POSS contents.

In addition to the DSC investigation on thermal properties, insight in thermomechanical properties has been tentatively pursued by dynamic mechanical thermal analysis (DMTA).

Before examining the results obtained, it is worth underlining that the nanoscale morphology of the films prepared for DMTA analysis, which were investigated by TEM, has been observed to be qualitatively similar to those of the corresponding composites previously reported. However, minor changes in the material micro- and nanostructure cannot be excluded and should be taken into account for a possible explanation of the poor reproducibility of DMTA measurements.

The spectra for storage modulus (E') and loss modulus (E'') for PSMA/POSS-NH_2 at different POSS concentrations, compared to those of neat PSMA, are given in Figure 7. PSMA clearly shows the α relaxation process with a peak of loss modulus (E'') at 115 °C: this value is related to T_g as determined by DSC, the difference between these two values being due to the different measurement conditions. Moreover, a weak and broad transition has been observed in the range between 65 and 85 °C, thus partially overlapping the α transition, as evidenced by the strongly asymmetric shape of E'' peak likely related to secondary chain relaxation of maleic anhydride groups. Significant differences in terms of α-relaxation temperature have been obtained for PSMA/POSS-NH_2 as compared to neat PSMA, depending on POSS loading. PSMA/POSS-NH_2 containing 5 and 10 wt % of POSS-NH_2 showed very similar results, with minor decrease of the elastic modulus plateau values and little delays of T_α toward higher temperatures (121 and 120 °C, respectively). These results might suggest a slight modification of molecular mobility by grafted POSS cages on the polymer backbone, thus hindering macromolecular mobility, either by inertial effect[59] or POSS−POSS associative interactions[60,61,9] despite this effect is not observable by DSC

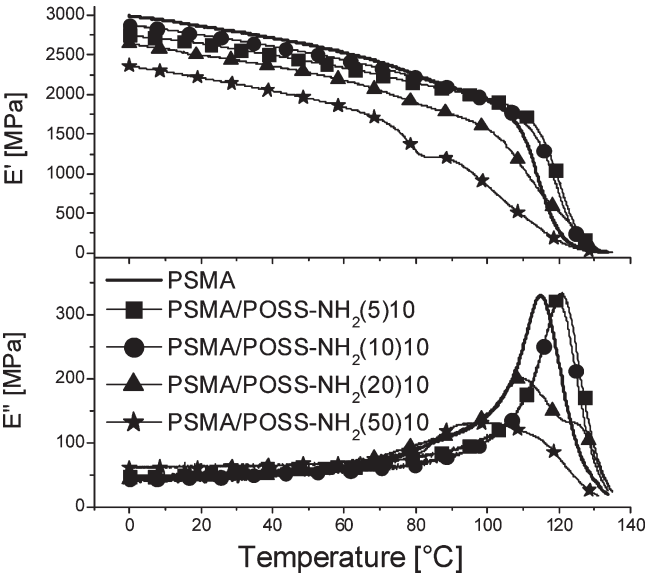

Figure 7. Storage modulus (E') and loss modulus (E'') plots for PSMA/POSS-NH_2, prepared with different POSS loadings. Mixing time: 10 min.

measurements. At higher POSS loadings, lower storage modulus and multiple relaxation peaks are observed, reflecting the complex multiphase structures described above for PSMA/POSS-NH_2 at 20 and 50% of POSS loadings, in agreement with the literature on multiphase polymers.[62−64] PSMA/POSS-NH_2(20)10 shows two main relaxations, observable as peaks in the E'' plot at ca. 109 and 125 °C. The above result reasonably correlates with the double glass transition observed in DSC, the lowest transition being related to the presence of plasticizing unbound POSS and the highest temperature signal being quite consistent with the DMTA results reported for PSMA/POSS-NH_2 containing 5 and 10% of POSS.

PSMA/POSS-NH_2(50)10 shows the lowest E' and E'' moduli over the whole temperature range and a very broad α-transition, centered at about 100 °C, which appears to be an overlapping of multiple peaks in the region between 90 and 120 °C. Moreover, a clear drop of the elastic modulus is observed for PSMA/POSS-NH_2(50)10 in the range between 60 and 80 °C, which appears to be related to the high excess of POSS, as evidenced by the low POSS grafting yield discussed above.

Kinetic Studies. In order to clarify the results obtained and assess the mechanism of composite system formation, some samples containing 20 wt % of POSS-NH_2 were prepared by applying different mixing times. SEM and TEM micrographs of the samples prepared are given in Figure 8. As far as the morphology of the composites prepared at low t_{mix} is concerned, SEM micrographs of the samples PSMA/POSS-NH_2(20)2 (t_{mix} = 2 min) and PSMA/POSS-NH_2(20)5 (t_{mix} = 5 min) show POSS aggregates on the polymer surface whose dimensions tend to decrease by increasing the mixing time. Indeed, PSMA/POSS-NH_2(20)2 holds POSS aggregates from 2 to 6 μm, while PSMA/POSS-NH_2(20)5 is characterized by POSS aggregates with smaller dimensions (from ca. 0.5 to 4 μm). As mentioned above (Figure 4), with increasing the mixing time the system surface becomes fully homogeneous at the microscale. Thus, for the samples prepared by using t_{mix} higher than 10 min, more detailed information on the morphological structure can be obtained by TEM measurements. PSMA/POSS-NH_2(20)10 (t_{mix} = 10 min), whose surface appears to be completely homogeneous

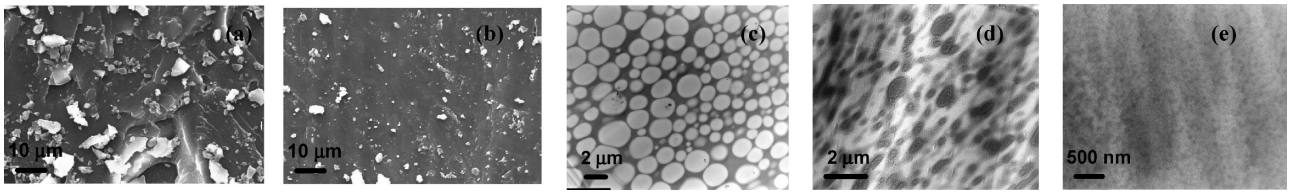

Figure 8. SEM micrographs of (a) PSMA/POSS-NH_2(20)2 and (b) PSMA/POSS-NH_2(20)5. TEM micrographs of (c) PSMA/POSS-NH_2(20)10, (d) PSMA/POSS-NH_2(20)20, and (e) PSMA/POSS-NH_2(20)30.

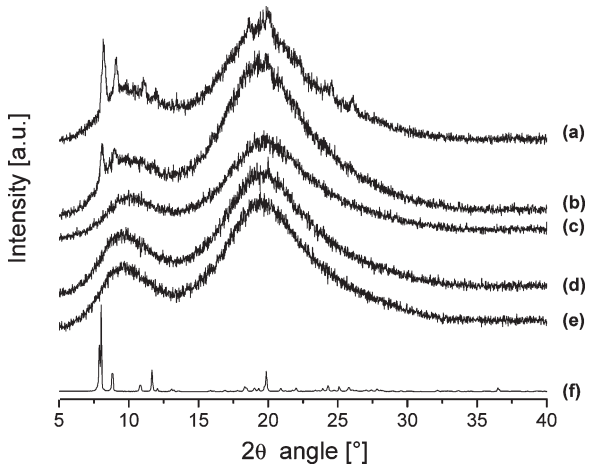

Figure 9. X-ray diffraction patterns of (a) PSMA/POSS-NH_2(20)2, (b) PSMA/POSS-NH_2(20)5, (c) PSMA/POSS-NH_2(20)10, (d) PSMA/POSS-NH_2(20)20, (e) PSMA/POSS-NH_2(20)30, and (f) POSS-NH_2. The curves are shifted vertically for clarity.

by SEM analysis, turns out to be characterized by a globular two-phase structure, holding different Si contents. A further evolution of the structure with increasing t_{mix} is evidenced by considering TEM micrographs of the samples PSMA/POSS-NH_2(20)20 (t_{mix} = 20 min) and PSMA/POSS-NH_2(20)30 (t_{mix} = 30 min). Indeed, PSMA/POSS-NH_2(20)20 holds dark globules, characterized by a higher Si content, into a continuous pale gray phase, thus evidencing a phase inversion as compared to PSMA/POSS-NH_2(20)10. This is likely due to progressive reaction of unbound POSS onto maleic anhydride functions and subsequent reduction of the fraction of free-POSS richphase below the critical value to behave as the continuous matrix. Further increasing the mixing time to 30 min, the structure observed by TEM is fully homogeneous at the submicrometer scale, with no evidence of residual phase separation. This fact suggests complete reaction of the POSS-NH_2, in agreement with grafting yield calculated by the extraction method.

WAXD characterization can provide further indications on the features of the samples prepared by varying the mixing time. In Figure 9, the WAXD spectra of the above-described samples are given together with that of the neat POSS-NH_2.

While the systems PSMA/POSS prepared at low mixing times, namely PSMA/POSS-NH_2(20)2 and PSMA/POSS-NH_2(20)5, show the typical silsesquioxane peaks (the most intense of them at ca. 2ϑ of 8.0° and 8.8°), PSMA/POSS-NH_2(20)10, PSMA/POSS-NH_2(20)20, and PSMA/POSS-NH_2(20)30 do not show any sharp diffraction peak.

The above findings confirm the morphological characterization results, giving evidence of a significant influence of the mixing time on the silsesquioxane dispersion in the polymer matrix.

Taking into account the results obtained and reminding that the temperature applied during POSS−polymer contact (240 °C) is lower than that of silsesquioxane melting temperature (260 °C), a surface reaction at the POSS crystal/polymer boundary is proposed. Indeed, POSS molecules on the surface of POSS crystals may react with the anhydride groups on the adjacent polymer backbone and subsequently be pulled away by the effect of mechanical mixing. The progressive decrease in size of crystalline POSS domains might be due, on one hand, to the surface reaction and from the other to the solubilization of silsesquioxane in the POSS-grafted PSMA, the latter becoming progressively more compatible than the virgin polymer matrix with POSS molecules upon the grafting process. Moreover, as evidenced by TEM characterization, a demixing between the fraction of the material containing different POSS concentration occurs.

As shown in Table 2, also the glass transition temperature has turned out to be affected by the mixing time. Indeed, while the samples PSMA/POSS-NH_2(20)2 and PSMA/POSS-NH_2(20)5, characterized by POSS aggregation, showed only a single T_g, similar to that of the polymer matrix, a secondary T_g at lower temperature (ca. 121 °C) has been found in the case of the systems showing compositional heterogeneity and the presence of unbound POSS. Conversely, PSMA/POSS-NH_2(20)30 did not show the low temperature T_g, being characterized by a uniform morphology and fully grafted POSS.

The effect of mixing time on thermomechanical properties has been also addressed by DMTA, showing that the multiple transitions described above for PSMA/POSS-NH_2(20)10 disappear when increasing the mixing time, so that a single peak is observed for both PSMA/POSS-NH_2(20)20 and PSMA/POSS-NH_2(20)30 at about 109 °C.

Film Preparation and Characterization. Among the possible applications, which can be envisaged, PSMA/POSS-NH_2 systems have been used to prepare dense films starting from acetone solutions. It is relevant to underline that while neat POSS-NH_2 is insoluble in the above solvent, the resulting composites turned out to be completely dissolved by acetone, even those based on high silsesquioxane content. Figure 10 shows the photographs of the films based on PSMA/POSS-NH_2(5)10 (Figure 10a) and PSMA/POSS-NH_2(20)10 (Figure 10b,c). Indeed, for the latter sample, two films have been prepared: one from the unwashed composite (Figure 10b) and the other from the sample which underwent a washing treatment accomplished to remove the unbound POSS (Figure 10c). While the film PSMA/POSS-NH_2(5)10 is completely transparent, that based on PSMA/POSS-NH_2-(20)10 turns out to be homogeneous but opaque. As shown in Figure 10c, for this sample the transparency can be obtained only by washing the pristine material. In order to explain these findings, it is necessary to take into account the nanoscale morphology of the films prepared from the sample PSMA/POSS-NH_2(20)10 which are, as previously reported, qualitatively similar to those reported for the composites. Indeed, both the pristine composites and the above films are characterized by a two-phase structure before the washing treatment, which clearly affects the light transmission through the film.

Table 2. Characteristics of the Samples Prepared by Applying Different Mixing Times

sample code	mixing time (min)	yield (%)	T_g bw[a] (°C)	T_g aw[b] (°C)
PSMA/POSS-NH_2(20)2	2	4	134	134
PSMA/POSS-NH_2(20)5	5	16	134	137
PSMA/POSS-NH_2(20)10	10	50	121, 135	137
PSMA/POSS-NH_2(20)20	20	84	121, 135	136
PSMA/POSS-NH_2(20)30	30	97	132	138

[a] Measurements carried out before washing the sample. [b] Measurements carried out after washing the sample.

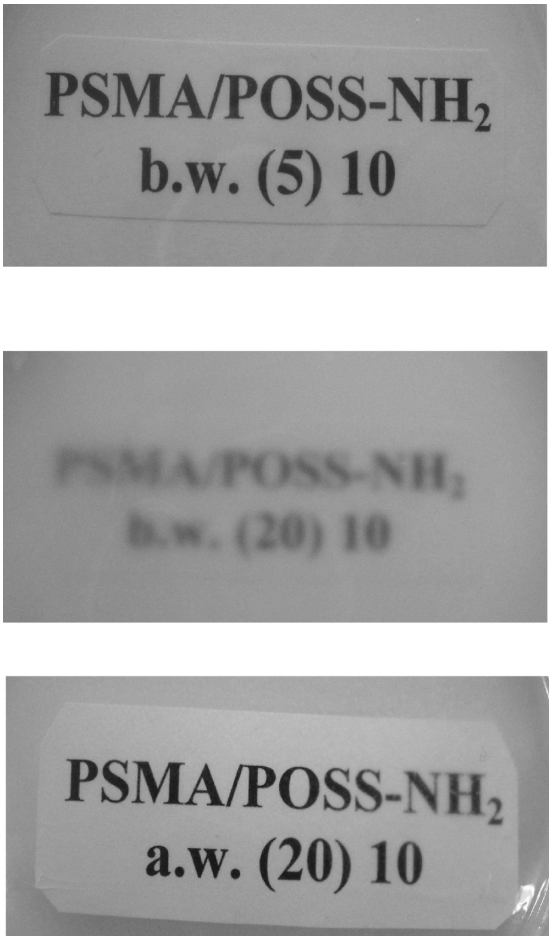

Figure 10. Dense films based on (a) PSMA/POSS-NH_2(5)10, (b) PSMA/POSS-NH_2(20)10, and (c) washed PSMA/POSS-NH_2(20)10.

In order to evaluate film wettability and address the influence of POSS on this property, contact angle measurements have been carried out. Indeed, while the contact angle of neat PSMA films is ca. 70°, that of those based on the composite systems turned out to be higher, being ca. 92°. Moreover, this value does not seem to depend on the washing treatment as well as on the POSS content. The influence of silsesquioxanes on surface properties has been previously evidenced on other POSS/polymer systems. Misra et al. found for PP/octaisobutyl-POSS nanocomposites an increase of surface hydrophobicity with respect to the neat polymer matrix.[65] The above finding has been explained by taking into account the cumulative effect of the eight hydrophobic isobutyl groups, attached to the POSS cage, as well as the increase of surface roughness of the nanocomposite films.

Similar considerations can be drawn also for our systems: namely, also in our case the increment of contact angle can be ascribed to the hydrophobic nature of silsesquioxane molecules, either grafted to the polymer chains or finely dispersed.

Conclusions

The preparation of PSMA/POSS hybrids with POSS loading up to 50 wt % has been carried out by one-step reactive melt blending, taking advantage of the grafting reaction of an amino-functionalized POSS on maleic anhydride groups.

Morphological analyses on these systems have shown POSS dispersion on the nanoscale, whereas the corresponding composites (obtained by the use of nonreactive POSS) presented residual micrometer-sized aggregates when processed in the same conditions.

The reaction mechanism has been assessed by means of FTIR measurements, evidencing the occurrence of the imidization reaction between MA group of PSMA and the amino group of POSS molecules, with the consequent formation of a cyclic imide linkage binding POSS to the polymer backbone. The grafting kinetics turned out to be controlled by a surface reaction at the POSS crystal/polymer boundary, the selected POSS being a solid in the used blending conditions. This led to the progressive evolution in time of the microstructure, passing from heterogeneous polymer/POSS mixture to biphasic polymer blends, where the two phases contain different concentrations of POSS, and finally to a fully homogeneous PSMA/POSS hybrid phase, corresponding to a complete grafting yield.

The phase separation has been found to control the thermal and thermomechanical properties of the material. In particular, multiple glass temperature transitions (T_g) and dynamo-mechanical relaxations (T_α) have been found, related to the presence of unbound POSS acting as a plasticizer, thus increasing molecular mobility of polymer chains. Surprisingly, no significant effects of grafted POSS have been observed in terms of thermal and thermomechanical properties: this is likely explained by the competing effects of molecular constraints due to the insertion of bulky Si−O−Si POSS cage and the free volume increase brought by the isobutyl organic substituents of POSS.

Excellent transparency of the PSMA/POSS hybrids has been observed, except in the case of biphasic systems, while the hybrids generally showed increased hydrophobicity, regardless of the amount of POSS in the explored concentration range.

Acknowledgment. The present study was supported by MIUR funds (PRIN 2006, Design and Synthesis of Multifunctional Polyhedral Silsesquioxanes for Novel Thermally Stable Polymer Composites). The authors acknowledge also the support of NoE "Nanofun Poly" for the diffusion of the research results.

References and Notes

(1) Kickelbick, G. In *Hybrid Materials, Synthesis, Characterisation and Applications*; Kickelbick, G., Ed.; Wiley-VCH Verlag: Weinheim, 2007; p 1.
(2) Sanchez, C.; Soler-Illia, G. J.; Ribot, F.; Lalot, T.; Mayer, C. R.; Cabuil, V. *Chem. Mater.* **2001**, *13*, 3061–3083.
(3) Sanchez, C.; Julian, B.; Belleville, P.; Popall, M. *J. Mater. Chem.* **2005**, *15*, 3559–3592.
(4) Kickelbick, G. *Prog. Polym. Sci.* **2003**, *28*, 83–114.
(5) Murugavel, R.; Walawalkar, M. G.; Dan, M.; Roesky, H. W.; Rao, C. N. R. *Acc. Chem. Res.* **2004**, *37*, 763–774.
(6) Harrison, P. G. *J. Organomet. Chem.* **1997**, *542*, 141–183.
(7) Baney, R. H.; Itoh, M.; Sakakibara, A.; Suzuki, T. *Chem. Rev.* **1995**, *95*, 1409–1430.
(8) Voronkov, M. G.; Lavrentyev, V. I. *Top. Curr. Chem.* **1982**, *102*, 199–236.
(9) Kopesky, E. T.; Haddad, T. S.; Cohen, R. E.; McKinley, G. H. *Macromolecules* **2004**, *37*, 8992–9004.
(10) Kopesky, E. T.; McKinley, G. H.; Cohen, R. E. *Polymer* **2006**, *47*, 299–309.

(11) Baldi, F.; Bignotti, F.; Fina, A.; Tabuani, D.; Riccò, T. *J. Appl. Polym. Sci.* **2007**, *105*, 935–943.
(12) Fina, A.; Abbenhuis, H. C. L.; Tabuani, D.; Camino, G. *Polym. Degrad. Stab.* **2006**, *91*, 2275–2281.
(13) Vannier, A.; Duquesne, S.; Bourbigot, S.; Castrovinci, A.; Camino, G.; Delobel, R. *Polym. Degrad. Stab.* **2008**, *93*, 818–826.
(14) Li, G.; Wang, L.; Ni, H.; Pittman, C. U. *J. Inorg. Organomet. Polym.* **2001**, *11*, 123−154 and references therein.
(15) Pittman, C. U.; Li, G.-Z.; Ni, H. *Macromol. Symp.* **2003**, *196*, 301–325.
(16) Phillips, S. H.; Haddad, T. S.; Tomczak, S. J. *Curr. Opin. Solid State Mater. Sci.* **2004**, *8*, 21–29.
(17) Pielichowski, K.; Njuguna, J.; Janowski, B.; Pielichowski, J. *Adv. Polym. Sci.* **2006**, *201*, 225–296.
(18) Fu, B. X.; Lee, A.; Haddad, T. S. *Macromolecules* **2004**, *37*, 5211–5218.
(19) Lee, A.; Xiao, J.; Feher, F. J. *Macromolecules* **2005**, *38*, 438–444.
(20) Carroll, J. B.; Waddon, A. J.; Nakade, H.; Rotello, V. M. *Macromolecules* **2003**, *36*, 6289–6291.
(21) Fu, B. X.; Yang, L.; Somani, R. H.; Zong, S. X.; Hsiao, B. S.; Phillips, S.; Blanski, R.; Ruth, P. *J. Polym. Sci., Part B: Polym. Phys.* **2001**, *39*, 2727–2739.
(22) Fu, B. X.; Gelfer, M. Y.; Hsiao, B. S.; Phillips, S.; Viers, B.; Blanski, R.; Ruth, P. *Polymer* **2003**, *44*, 1499–1506.
(23) Fina, A.; Tabuani, D.; Frache, A.; Camino, G. *Polymer* **2005**, *46*, 7855–7866.
(24) Zhao, Y.; Schiraldi, D. A. *Polymer* **2005**, *46*, 11640–11647.
(25) Fina, A.; Tabuani, D.; Camino, G. In *Nanostructured and Functional Polymer-based Materials and Nanocomposites*; Lazzari, M., Kenny, J. M., Camino, G., Mijangos, C., Eds.; Universidade de Santiago de Compostela: Santiago de Compostela, 2007; p 80.
(26) Yoon, K. H.; Polk, M. B.; Park, J. H.; Min, B. G.; Schiraldi, D. A. *Polym. Int.* **2005**, *54*, 47–53.
(27) Zeng, J.; Kumar, S.; Iyer, S.; Schiraldi, D. A.; Gonzalez, R. I. *High Perform. Polym.* **2005**, *17*, 404–424.
(28) Zhou, Z.; Cui, L.; Zhang, Y.; Zhang, Y.; Yin, N. *Eur. Polym. J.* **2008**, *44*, 3057–3066.
(29) Zhou, Z.; Cui, L. M.; Zhang, Y.; Zhang, Y.; Yin, N. *J. Polym. Sci., Part B: Polym. Phys.* **2008**, *46*, 1762–1772.
(30) Zhou, Z.; Zhang, Y.; Zhang, Y.; Yin, N. *J. Polym. Sci., Part B: Polym. Phys.* **2008**, *46*, 526–533.
(31) Choi, J.-H.; Jung, C.-H.; Kim, D.-K.; Ganesan, R. *Nucl. Instrum. Methods B* **2008**, *266*, 203–206.
(32) Fina, A.; Tabuani, D.; Peijs, T.; Camino, G. *Polymer* **2009**, *50*, 218–226.
(33) Fina, A.; Tabuani, D.; Carniato, F.; Frache, A.; Boccaleri, E.; Camino, G. *Thermochim. Acta* **2006**, *440*, 36–42.
(34) Fina, A.; Tabuani, D.; Frache, A.; Boccaleri, E.; Camino, G. In *Fire Retardancy of Polymers: New Applications of Mineral Fillers*; Le Bras, M., Wilkie, C., Bourbigot, S., Eds.; Royal Society of Chemistry: Cambridge, UK, 2005; pp 202−220.
(35) Boyer, C.; Boutevin, B.; Robin, J. *Polym. Degrad. Stab.* **2005**, *90*, 326–339.
(36) Lichtenhan, J. D.; Otonari, Y. A.; Carr, M. J. *Macromolecules* **1995**, *28*, 8435–8437.
(37) Mather, P. T.; Jeon, H. G.; Romo-Uribe, A.; Haddad, T. S.; Lichtenhan, J. D. *Macromolecules* **1999**, *32*, 1194–1203.
(38) Fu, B. X.; Hsiao, B. S.; Pagola, S.; Stephens, P.; White, H.; Rafailovich, M.; Sokolov, J.; Mather, P. T.; Jeon, H. G.; Phillips, S.; Lichtenhan, J.; Schwab, J. *Polymer* **2001**, *42*, 599–611.
(39) Zheng, L.; Waddon, A. J.; Farris, R. J.; Coughlin, E. B. *Macromolecules* **2002**, *35*, 2375–2379.
(40) Kim, B.-S.; Mather, P. T. *Macromolecules* **2006**, *39*, 9253–9260.
(41) Zheng, L.; Hong, S.; Cardoen, G.; Burgaz, E.; Gido, S. P.; Coughlin, E. B. *Macromolecules* **2004**, *37*, 8606–8611.
(42) Seurer, B.; Coughlin, E. B. *Macromol. Chem. Phys.* **2008**, *209*, 1198–1209.
(43) Fu, B. X.; Lee, A.; Haddad, T. S. *Macromolecules* **2004**, *37*, 5211.
(44) Liu, L.; Tian, M.; Zhang, W.; Zhang, L.; Mark, J. E. *Polymer* **2007**, *48*, 3201–3212.
(45) Pyun, J.; Matyjaszewski, K.; Wu, J.; Kim, G.-M.; Chun, S. B.; Mather, P. T. *Polymer* **2003**, *44*, 2739–2750.
(46) Ricco, L.; Russo, S.; Monticelli, O.; Bordo, A.; Bellucci, F. *Polymer* **2005**, *46*, 6810–6819.
(47) Ríos-Dominguez, H.; Ruiz-Treviño, F. A.; Contreras-Reyes, R.; González-Montiel, A. *J. Membr. Sci.* **2006**, *271*, 94–100.
(48) Liu, Y.; Zheng, S.; Nie, K. *Polymer* **2005**, *46*, 12016–12025.
(49) Liu, Y. R.; Huang, Y. D.; Liu, L. *Polym. Degrad. Stab.* **2006**, *91*, 2731–2738.
(50) Liu, Y. R.; Huang, Y. D.; Liu, L. *Compos. Sci. Technol.* **2007**, *67*, 2864–2876.
(51) Sinha Ray, S.; Okamoto, M. *Prog. Polym. Sci.* **2003**, *28*, 1539–1641.
(52) Bharadwaj, R. K.; Berry, R. J.; Farmer, B. L. *Polymer* **2000**, *41*, 7209.
(53) Lee, A.; Lichtenhan, J. D. *Macromolecules* **1998**, *31*, 4970–4974.
(54) Romo-Uribe, A.; Mather, P. T.; Haddad, T. S.; Lichtenhan, J. D. *J. Polym. Sci., Part B: Polym. Phys.* **1998**, *36*, 1857.
(55) Li, G. Z.; Wang, L.; Toghiani, H.; Daulton, T. L.; Koyama, K.; Pittman, C. U.Jr. *Macromolecules* **2001**, *34*, 8686.
(56) Xu, H.; Kuo, S.-W.; Lee, J.-S.; Chang, F.-C. *Polymer* **2002**, *43*, 5117–5124.
(57) Wu, J.; Haddad, T. S.; Kim, G.-M.; Mather, P. T. *Macromolecules* **2007**, *40*, 544–554.
(58) Markovic, E.; Clarke, S.; Matisons, J.; Simon, G. P. *Macromolecules* **2008**, *41*, 1685–1692.
(59) Romo-Uribe, A.; Mather, P. T.; Haddad, T. S.; Lichtenhan, J. D. *J. Polym. Sci., Part B: Polym. Phys.* **1998**, *36*, 1857–1872.
(60) Wientjes, R. H. W.; Jongschaap, R. J. J.; Duits, M. H. G.; Mellema, J. *J. Rheol.* **1999**, *43*, 375–391.
(61) Fu, B. X.; Gelfer, M. Y.; Hsiao, B. S.; Phillips, S.; Viers, B.; Blansky, R.; Ruth, P. *Polymer* **2003**, *44*, 1499–1506.
(62) Pinoit, D.; Prud'homme, R. E. *Polymer* **2002**, *43*, 2321–2328.
(63) Ahmad, Z.; Al-Awadi, N. A.; Al-Sagheer, F. *Polym. Degrad. Stab.* **2007**, *92*, 1025–1033.
(64) De Lima, J. A.; Felisberti, M I. *Eur. Polym. J.* **2008**, *44*, 1140–1148.
(65) Misra, R.; Fu, B. X.; Morgan, S. E. *J. Polym. Sci., Part B: Polym. Phys.* **2007**, *45*, 2441–2455.